Structures and Buildings
Volume 168 Issue SB10

Role of hoops on seismic performance of reinforced concrete joints
Dhake, Patil and Patil

ice | proceedings

Proceedings of the Institution of Civil Engineers
Structures and Buildings 168 October 2015 Issue SB10
Pages 708–717 http://dx.doi.org/10.1680/stbu.14.00107
Paper 1400107
Received 02/11/2014 Accepted 27/03/2015
Published online 20/07/2015
Keywords: anchors & anchorages/buildings, structures & design/seismic engineering

ice Institution of Civil Engineers publishing

Role of hoops on seismic performance of reinforced concrete joints

1 Pravinchandra D. Dhake ME
Research Scholar, Applied Mechanics Department, SVNIT-Surat, Gujrat, India

2 Hemant S. Patil PhD
Professor, Applied Mechanics Department, SVNIT-Surat, Gujrat, India

3 Yogesh D. Patil PhD
Assistant Professor, Applied Mechanics Department, SVNIT-Surat, Gujrat, India



Four exterior reinforced concrete beam–column joint specimens with varying amounts of joint hoop reinforcement are constructed and tested under reverse cyclic loading to assess their performance during earthquakes. Headed bars are used in all the specimens. Various parameters such as crack pattern, hysteresis behaviour, modes of failure, energy dissipation, displacement ductility, stiffness degradation and maximum shear strength are studied. The effectiveness of headed bars with short embedded length terminating in the exterior beam–column joint is assessed. As headed bars have the advantage of transferring a more uniform distribution of compressive stress to the concrete at the headed end, they enable the development of a wider compressive strut in the joint, which enhances the joint shear strength under seismic loading. This makes it possible to reduce transverse reinforcement in joints when using headed bars as longitudinal beam reinforcement.

Notation

A_b	bar area (mm^2)
A_{brg}	net bearing area (mm^2)
A_{ch}	cross-sectional area of a structural member measured out-to-out of transverse reinforcement (mm^2)
A_g	gross area of cross-section (mm^2)
A_{head}	gross head area (mm^2)
A_j	effective cross-sectional area within joint (mm^2)
A_{obs}	area of obstruction (mm^2)
A_{st}	area of tension reinforcement of beam (mm^2)
b_c	core dimension perpendicular to tie legs measured to outside edges of transverse reinforcement (mm)
d_b	bar diameter (mm)
f'_c	specified concrete cylinder strength (MPa)
f_y	specified strength of headed bar (MPa)
f_{yt}	yield strength of hoop reinforcement (MPa)
j	internal lever arm factor
L_b	length of beam from column (mm)
L_c	distance between column inflection points (mm)
l_{dt}	development length in tension (mm)
M_n	nominal flexural strength (kN)
P_{max}	ultimate load (kN)
P_n	nominal flexural load (kN)
s_h	spacing of hoop reinforcement (mm)
T	tensile force in the beam reinforcement
T_{max}	maximum tensile force in longitudinal reinforcement of beam
V_{col}	horizontal column shear
$V_{jh,\ test}$	maximum joint shear
V_n	nominal shear strength
γ	constant depends upon connection classification
Δ_{max}	ultimate displacement (mm)
Δ_{max}/Δ_y	displacement ductility
Δ_y	yield displacement (mm)
μ	displacement ductility
Ψ_e	factor based on reinforcement coating

1. Introduction

Construction of any structure that is designed and detailed to withstand seismic forces requires congested reinforcement configuration. Anchorage is the fundamental principle that underlines the behaviour and strength of external beam–column joints, and which defines the rigidity of the joint. Anchorage is achieved through a combination of bond (adhesion, friction

and bearing against transverse ribs) and bearing on hooks. Standard 90° and 180° hooks at the exterior beam–column joints become unmanageable and are not feasible when dimensions of the connecting members are restricted. Increasing use of high-strength concrete in a structure results in smaller cross-sections, which aggravates problems of congestion. Previous research has shown that the use of headed bars can be the most feasible and practicable alternative to reduce development lengths of the bars, and anchor the bar effectively within the beam–column junction (Bashandy, 1996; Wallace *et al.*, 1998; Wright and McCabe, 1997). Use of high-strength steel makes this problem more critical. Headed bars alleviate complications while laying reinforcement, placement and compaction of concrete (Chun *et al.*, 2007). To study the parameters influencing the behaviour of mechanical anchorage, research has been conducted on idealised evaluations where headed bars were pulled from concrete blocks (Wright and McCabe, 1997) and columns (Bashandy, 1996; Chun *et al.*, 2009). By using actual specimens of beam–column joints, the experimental work was conducted to assess the effectiveness of headed bars with the emphasis on joint detailing (Chun *et al.*, 2007; Wallace *et al.*, 1998) and small head size (Kang *et al.*, 2010). The anchorage strength of headed bars with short development lengths has been investigated (Dhake *et al.*, 2015). Anchoring the longitudinal reinforcement of the beam by using steel plates has been found to minimise cracking and deformation of the joints (Kotsovou and Mouzakis, 2011). Limited research has been conducted on the role of joint hoops within the beam–column junctions with headed bars. The embedded length of the headed bar increases the anchorage capacity of the headed bar. With limited anchorage length, the same anchorage capacity can be obtained by using transverse reinforcement, since it provides a clamping force on the concrete in which the headed bars are anchored. Transverse shear reinforcement is used to enhance the anchorage capacity of headed bars by confining the concrete and to carry joint shear. The amount of joint hoops to fulfill this function affects the detailing at the joint.

2. Research significance

ACI codes (ACI 318-08 (ACI, 2008) and ACI 352R (ACI-ASCE, 2002)) specify requirements for minimum area of joint transverse reinforcement and maximum permissible spacing of transverse reinforcement to obtain adequate concrete confinement. This increases steel congestion, which leads to difficulty in fabrication and concrete placement. For joints with headed bars, no separate provision for joint transverse reinforcement is given by codes. The anchorage capacity of a headed bar is largely attributable to its bearing, which may require less confinement as compared to a joint with hook bars.

An experimental study was devised to investigate the role of joint hoops in the shear strength of exterior beam–column joints with headed bars subjected to reverse cyclic loading.

Four exterior beam–column joint specimens with varying amounts of joint shear reinforcement (joint hoops) were constructed and tested. Headed bars were used in all the specimens. The various parameters such as crack pattern, hysteresis behaviour, modes of failure, energy dissipation, displacement ductility, stiffness degradation and maximum shear strength were studied.

3. Development length and details of headed bars

The net bearing area A_{brg} is defined as the gross head area A_{head} minus the area of obstruction A_{obs}. Previous experimental research has shown that a ratio (A_{brg}/A_b) of approximately 4 is appropriate to ensure proper anchorage (Chun *et al.*, 2007; Dhake *et al.*, 2015; Thompson *et al.*, 2005) and the same is recommended by ACI 318-08 (ACI, 2008) as the minimum head size. Hence, bars with circular heads with (A_{brg}/A_b) = 4 were used in the present study.

As per ACI 352R-02 (ACI-ASCE, 2002), the development length in tension (l_{dt}) for headed bars is defined as

1. $$l_{dt} = \frac{0 \cdot 179 f_y d_b}{\sqrt{f'_c}} \quad \text{for type 1 joint}$$

2. $$l_{dt} = \frac{0 \cdot 15 f_y d_b}{\sqrt{f'_c}} \quad \text{for type 2 joint}$$

In Equation 2 the stress multiplier 1·25 is considered to account for over-strength and strain-hardening of reinforcement. This provision defines a type 1 connection as the connection which has members that are designed to satisfy strength requirements without significant inelastic deformation. Furthermore, it defines a type 2 connection as the connection which has members required to dissipate energy through reversals of deformation into the inelastic range. The length should be measured from the back face of the head plate to the beam interface for a type 1 connection, whereas, for a type 2 connection, it is measured up to the outer face of the joint hoop only.

ACI 318-08 (ACI, 2008) also defines the development length in tension (l_{dt}) for headed bars as follows

3. $$l_{dt} = \frac{0 \cdot 19 \psi_e f_y d_b}{\sqrt{f'_c}} \geq \text{the larger of } 8d_b \text{ and } 152 \text{ mm}$$

The length is measured from the inner face of the head plate to the beam–column interface, where f_y is the specified strength of a headed bar (MPa); f'_c is the specified concrete cylinder

strength (MPa); d_b is the bar dia. (mm); and $\Psi_e = 1{\cdot}2$ for epoxy-coated bars and 1·0 for other cases. For the measured material properties of the present experimental work the development length works out to be $17d_b$ as per Equation 1, $14{\cdot}2d_b$ as per Equation 2 and $18d_b$ as per Equation 3.

4. Hoop reinforcement and shear strength

As per ACI 318-08 (section 21·7·4) (ACI, 2008), nominal shear strength (V_n) is based on

$$4. \quad V_n = 0 \cdot 083\gamma\sqrt{f'_c}A_j$$

where A_j is the effective cross-sectional area within a joint in a plane parallel to the plane of reinforcement; constant γ depends on connection classification – for an inter-storey exterior beam–column junction, its value is 12. The code evaluates the nominal shear capacity based on the strut mechanism and expresses it as a function of concrete strength, irrespective of the amount of shear reinforcement. However, the code requires a minimum amount of transverse reinforcement in the joint to confine the joint and for necessary force transfer within the joint. As per ACI 318-08 (section 21·6·4) (ACI, 2008), the minimum total cross-sectional area of rectangular hoop reinforcement should be not less than that required by Equations 5 and 6

$$5. \quad A_{sh} = \frac{0 \cdot 3 s_h b_c f'_c}{f_{yt}} \left(\frac{A_g}{A_{ch}} - 1 \right)$$

$$6. \quad A_{sh} = \frac{0 \cdot 09 s_h b_c f'_c}{f_{yt}}$$

where s_h is the spacing hoop reinforcement; b_c is the core dimension perpendicular to the tie legs measured to the outside edges of the transverse reinforcement; f_{yt} is the yield strength of hoop reinforcement; A_g is the gross area of column section; and A_{ch} is the cross-sectional area of a structural member measured out-to-out of transverse reinforcement. The values for ratio of provided A_{sh} to the minimum required A_{sh} as per Equations 5 and 6 are given later in Table 2. ACI 318-08 (ACI, 2008) also specifies requirements for maximum permissible spacing of transverse reinforcement to obtain adequate concrete confinement.

Based on the capacity design concept, the design shear force, $V_{jh,u}$ can be estimated by using

$$7. \quad V_{jh,u} = T - V_{col} = 1 \cdot 25 \left(A_{st} f_y - A_{st} f_y \frac{jd}{L_c} \right)$$

where T is the tensile force in the beam reinforcement; V_{col} is the horizontal column shear; 1·25 is the over strength factor; A_{st} is the area of tension reinforcement of the beam; f_y is the specified yield strength of the beam longitudinal reinforcement; L_c is the distance between column inflection points; and jd is the internal lever arm of the beam section (approximately 7/8 of the effective depth of the beam).

5. Experimental investigations

5.1 Material properties

The concrete mix was designed for M30 grade with medium workability. Pozzolana Portland cement (PPC) of 53 grade conforming to IS 1489: Part I (BIS, 1991) and natural river sand with specific gravity 2·69 and fineness modulus 3·5 which conforms to grading zone II (IS 383 (BIS, 1970)) were used as fine aggregate. Crushed basalt with maximum size of 20 mm and specific gravity 2·79 was used as course aggregate. Thermo-mechanically treated iron (Fe) 500 grade ribbed bars of 12 mm dia. (here denoted in the diagrams as #12) were used as longitudinal reinforcement of beams and columns, whereas 6 mm dia. bars (denoted as #6 in the diagrams) were used as transverse reinforcement. Three bars were tested for mechanical properties; the 0·2% proof stress of #12 bars was in the range of 520–530 MPa and that of #6 was 500 MPa. Figure 1 shows the stress–strain curves of reinforcing steel.

5.2 Details of specimens

The dimensions and reinforcement details of the specimens are shown in Figure 2. The total height of the column (distance between top and bottom hinge points) in all the specimens was 900 mm. The lengths of columns and beams were defined to simulate the nearest inflection points in the beam and column framing into the joint. In all the specimens, the main

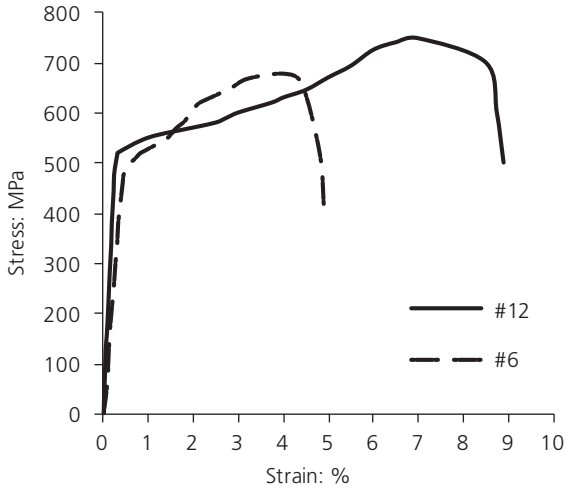

Figure 1. Stress–strain curve for reinforcement steel

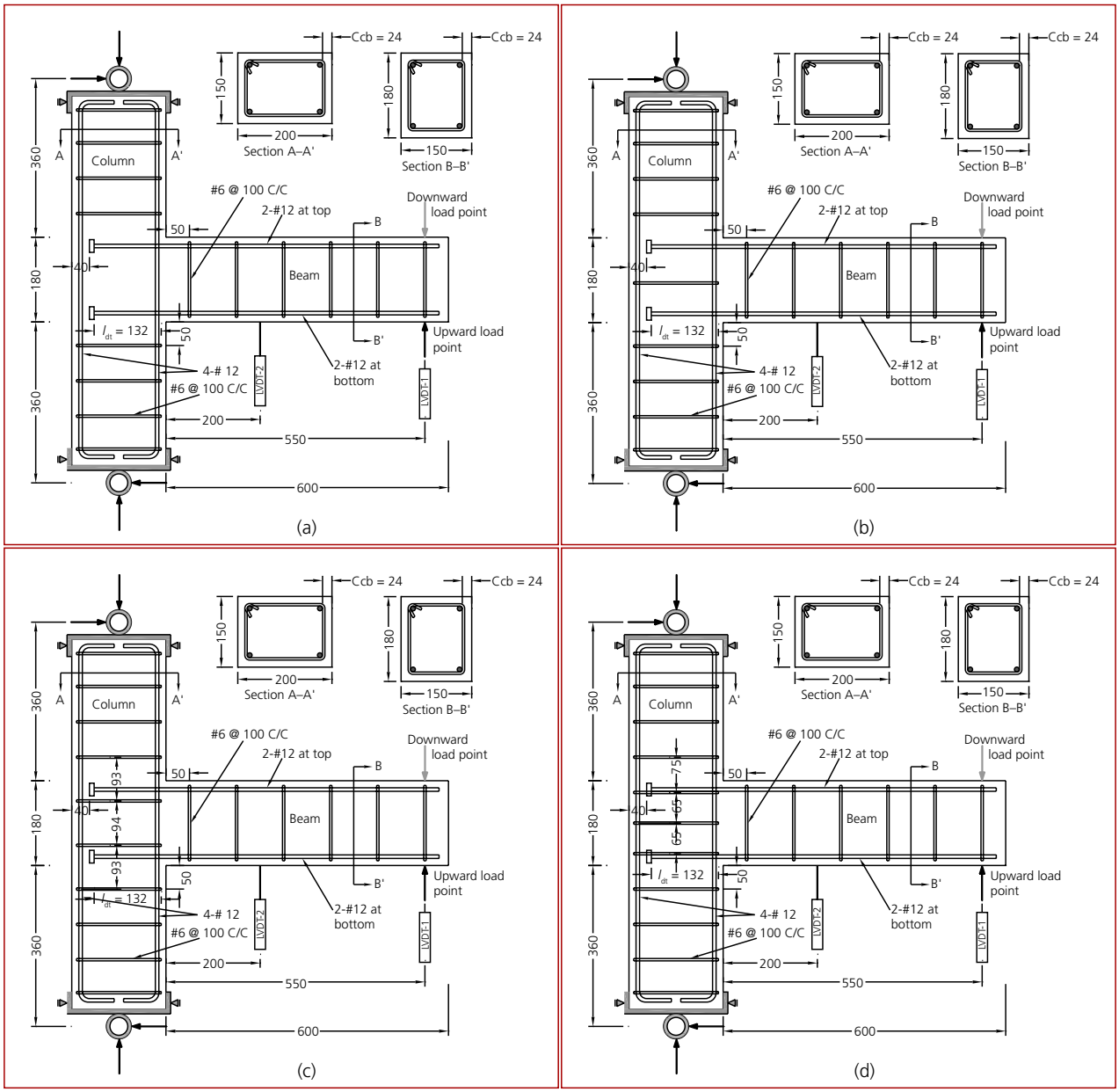

Figure 2. Reinforcement details of specimens: (a) J4; (b) J7; (c) J8; (d) J9

reinforcement provided in the beam was two 12 mm dia. bars at the top and two 12 mm dia. bars at the bottom, whereas in the column, four 12 mm dia. bars were provided. In the beam, centre-to-centre stirrups 6 mm in diameter at 100 mm were provided, and in the columns were 6 mm diameter at 100 mm centre-to-centre ties. Clear cover for all headed bars was $2d_b$.

In the present research work the column depth was considered as 200 mm so that available development length was $11d_b$ ($\approx 0 \cdot 12 f_y d_b / \sqrt{f'_c}$), which is measured from the inner face of the head plate to the outer face of the joint hoop (see Figure 2). The development length provided within the joints in all specimens was 83% of that required by ACI 352R-02 (ACI-ASCE, 2002) (type 2 joint), whereas it was 69% of that required by ACI 318-08 (ACI, 2008). Although a short development length was available, the heads were placed in the zone of the diagonal compression strut. A headed bar was formed by inserting the end portion of a straight reinforcing bar into the centrally drilled hole of a 10-mm-thick, circular plate, and welding it at both the faces of the plate. To investigate the contribution of concrete to anchorage strength, transverse

reinforcement was not placed in the joint in specimen J4. Total area of transverse reinforcement placed in specimen J9 was approximately equal to the minimum area (A_{sh}) specified by ACI 318-08 (ACI, 2008). The amount of joint hoops was decreased in specimens J7 and J8. 16% and 50% of minimum A_{sh} specified by ACI 318-08 (ACI, 2008) were provided in specimens J7 and J8, respectively. The provisions of maximum spacing are not considered while providing joint hoops to avoid congestion at the joint.

5.2.1 Casting and curing

All the specimens were cast horizontally rather than vertically, as in actual construction practice. The concrete was placed into the mould immediately after mixing and well compacted. Control cubes and cylinders were prepared along with the concreting of specimens. The moulds were removed 24 h after casting. After 28 d of curing, the specimens were dried in air and white-washed so as to improve crack visibility.

5.3 Test set-up and instrumentation

The test set-up is shown in Figure 3. The specimens were tested in a reaction frame. Each of the test specimens was subjected to cyclic load reversals to simulate earthquake loadings. A 1000 kN capacity calibrated hydraulic jack, mounted vertically on the frame, was used to apply axial load on the column. The critical condition for a beam–column joint is when it is subjected to seismic forces without any axial load. But in reinforced concrete the dead load component is so large that the columns are always subjected to a certain amount of axial force. Hence a constant load of 100 kN, which is about 20% of the axial capacity of the column, was applied to the

Figure 3. Test set-up

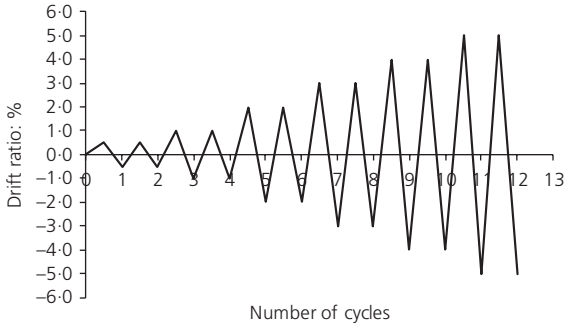

Figure 4. Loading regime

columns to hold the specimens in position and to simulate column axial load. Two ends of the column were given an external axial hinge support in addition to lateral hinge support provided at the top and bottom of the column. Another two 500 kN capacity hydraulic jacks were used to apply reverse cyclic loading. The load was applied at a distance of 50 mm from the free end of the beam face. The load was measured by inserting a load cell in between the jack and the beam face. The test was displacement (drift ratio) controlled and the specimen was subjected to an increasing cyclic displacement – where the drift ratio (DR) is defined as the ratio of deflection Δ of the load point to the distance between the load point and the centre-line of the column. Figure 4 shows the loading regime in terms of applied cycles plotted against storey drift ratio. The deflections were measured by linear variable differential transducers (LVDTs) at the beam free end tip (at loading point), at distance 200 mm from the beam–column junction.

6. Test results and discussion

6.1 Modes of failure and cracking behaviour

Three modes of failure were established. Joint shear failure (JF) was characterised by gradual loss of load-carrying capacity before the formation of the plastic hinge in the adjacent beam. Beam flexure failure (BF) was identified by gradual loss of load-carrying capacity after the formation of a plastic hinge in the region of the beam adjacent to the joint. The combined mode of failure was denoted by BJF. The crack patterns for all the specimens at the end of the test are shown in Figures 5(a)–5(d). All of the sections were reinforced with equal top and bottom reinforcement. During upward loading the bottom reinforcement yielded in tension. During the initial stages of reloading, since the cracks were open, the concrete did not contribute to carrying the compressive force. Obviously compression reinforcement was vital in carrying these compressive forces. After closure of cracks, the total compressive force was shared between concrete and reinforcement, therefore the member became stiffer as compared to the initial stages of the loading cycle. However, imperfect closure of

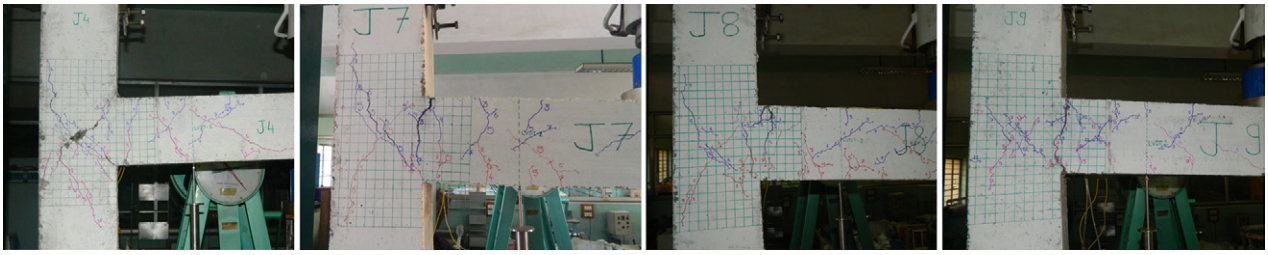

Figure 5. Crack pattern of specimens: (a) J4; (b) J7; (c) J8; (d) J9

cracks due to debris and shear displacements, in combination with the Bauschinger effect, result in a noticeable stiffness degradation as compared to previous cycles (Park and Paulay, 1974; Scarpas, 1981).

In specimen J4, the initial joint shear cracks appeared diagonally during DR 1·0%. In the subsequent cycles, the initial cracks widened and propagated further up to DR 3%, and some new cracks also appeared at DR 2%. All the cracks appeared diagonally at the joint region. Although some cracks were observed in the beam length, no cracks were observed at the beam interface. A typical 'x' cracks pattern was observed, since no joint hoops were provided at the joint. Spalling of concrete along the diagonal cracks was observed during DR 4%, which was the cumulative effect of opening of diagonal tension cracks and the crushing of diagonal compression struts.

In specimen J7, initial cracks appeared at the beam interface during DR 0·5%, which propagated and widened in the subsequent cycles. The diagonal cracks were initiated at DR 2%, which extended along the diagonal up to DR 3%. Many other cracks also appeared across the joint region and in the beam length. It was observed that the width of the diagonal cracks was less at the centre of the joint panel, since a joint hoop was provided at this location. The widths of the diagonal cracks were more in the upper half and lower half portions of the joint panel where joint hoops were not provided. Specimen J7 incorporated damage in the joint region owing to shear cracks, as well as in the beam region near the interface.

The initial pattern of cracks in specimen J8 is the same as that of specimen J7. Above DR 3%, the width of the crack at the beam interface increased, whereas the width of the diagonal crack remained constant. Finally, the failure of the specimen was due to the formation of a plastic hinge at the beam interface.

The shear strength of specimen J9 was very significant, as initial cracks developed in the joint in the fifth to the seventh cycles, but deformation occurred in the beam owing to the progressive increase of crack width at the beam interface, and some more cracks in the length of the beam. The crack controlling ability of specimen J8 was slightly superior to that of specimen J7, but remarkable crack controlling ability was exhibited by specimen J9. Failure of the joint core was prevented partly in specimen J7, considerably in specimen J8, and completely in specimen J9. No sign of side blowout was observed in any specimen, even where transverse reinforcement was not provided. Hence clear cover to the headed bar of $2d_b$ is sufficient to prevent side blowout. In all the specimens the head plate was placed at 40 mm from the exterior face of column. No signs of punching shear failure were observed during the testing. This means that the compression developed in the compression zone bar is less than the punching shear resisting capacity of concrete cover provided to the head plate.

6.2 Hysteretic performance

The load plotted against displacement graphs–hysteresis loops are shown in Figures 6(a)–6(d). Specimen J4, although it failed in the joint, exhibited a satisfactory hysteretic response up to DR 3%. This observation highlighted that a certain level of performance can be achieved with headed bars even without joint hoop reinforcement. In all the specimens, it was observed that the repeated loading cycle dissipated less energy than the primary loading cycle for each respective DR. The hysteresis loops for specimens J8 and J9 are wide and stable, with higher energy dissipation in each primary loading cycle.

6.3 Energy dissipation

The energy dissipated at the beam–column joint specimens through plastic deformation was the sum of the area in the beam tip load–displacement hysteresis loop. The cumulative dissipated energy of all specimens is given in Table 1 and Figure 7.

The energy dissipated by specimen J4 is less than 50% of that of J9. Up to DR 4% the energy dissipated by specimens J8 and J9 was almost the same. At the next DR for specimen J8, the peak load of the cycle decreased considerably and, hence, the test was stopped. The best energy dissipation potential was exhibited by specimen J9, as the formation of the complete plastic hinge took place at the beam–column interface.

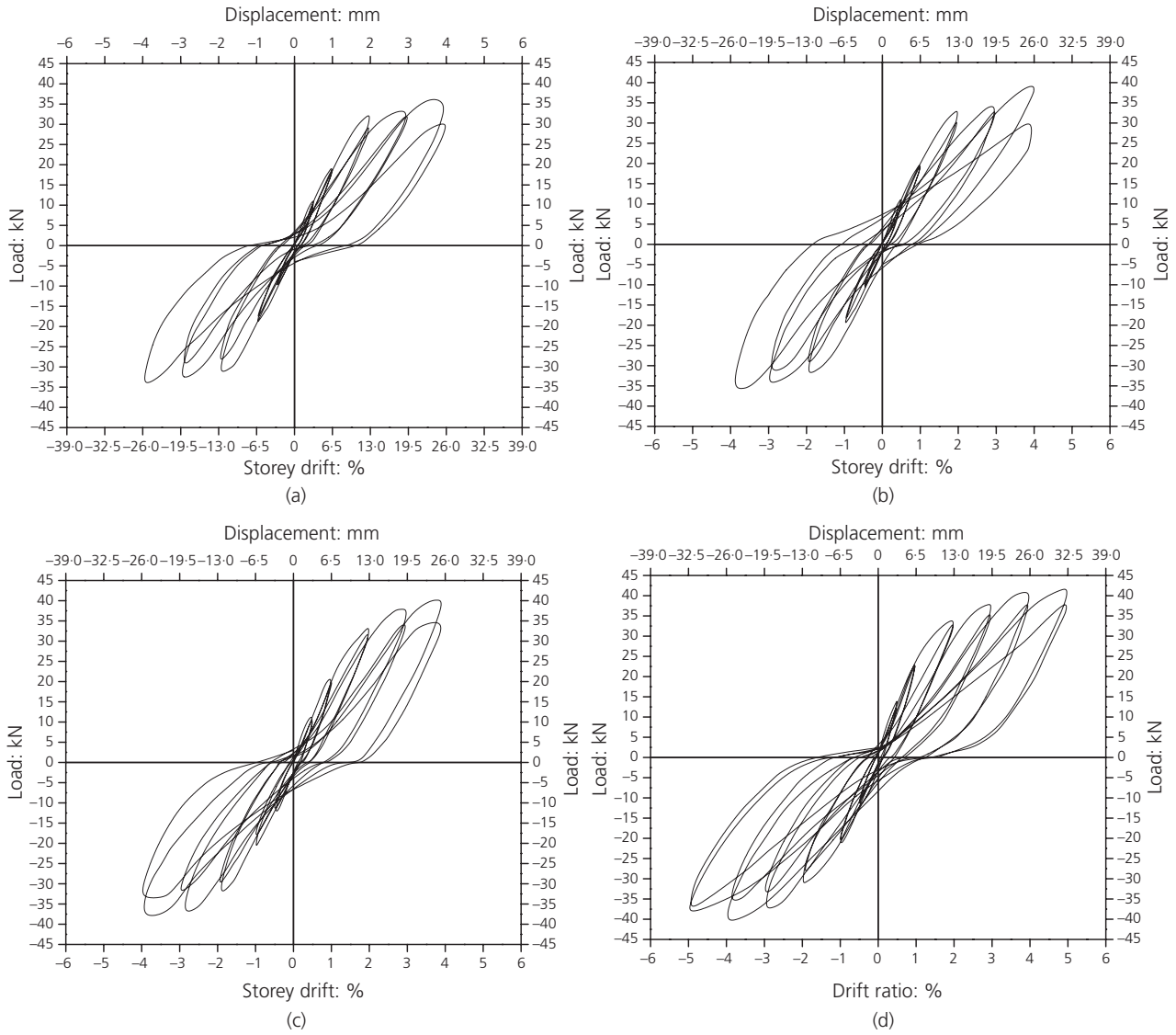

Figure 6. Load–displacement hysteresis loops of specimens: (a) J4; (b) J7; (c) J8; (d) J9

Specimen	Nominal flexural strength, M_n: kN m	Yield displacement, Δ_y: mm	Displacement ductility, Δ_{max}/Δ_y	Stiffness: kN/mm		Energy dissipation: kN mm
				Initial	Final	
J4	15·63	7·73	3·36	3·42	1·39	2000
J7	15·63	7·33	3·55	3·51	1·43	2357
J8	15·63	6·67	3·9	3·75	1·32	2633
J9	15·63	6·0	5·42	4·14	1·16	4293

Table 1. Nominal flexural strengths, displacement ductility, stiffness and energy dissipation of specimens

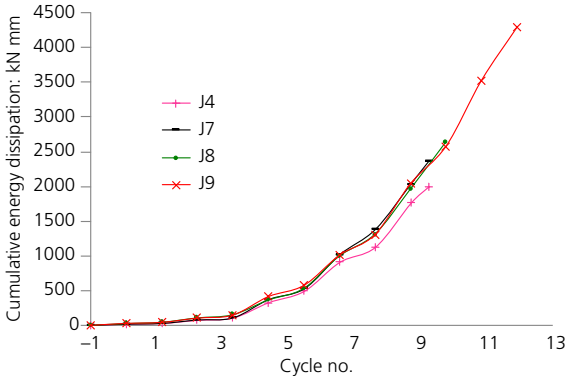

Figure 7. Cumulative energy dissipation

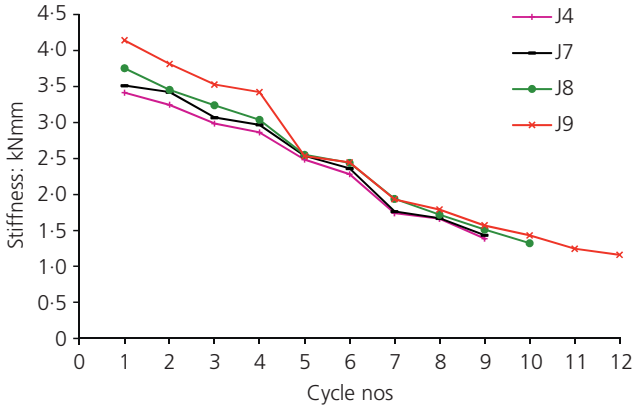

Figure 8. Stiffness degradation of test specimens

The decrease in joint shear reinforcement by 33% (J8), 66% (J7) and 100% (J4) caused decrease in energy dissipation by 39%, 45% and 53%, respectively.

6.4 Displacement ductility

Nominal flexural strength (M_n) was predicted for each specimen. The nominal flexural strength was defined as the force at which beam yielding would occur when the contribution of reinforcement in the compression zone and the measured material properties were used in the analysis. In both the cases, partial safety factors for materials were not considered. The test day compressive strength of control concrete cubes and cylinders was 35 MPa and 30 MPa, respectively.

The displacement ductility (μ) is defined as Δ_{max}/Δ_y, where Δ_{max} is the vertical displacement at the loading point of the beam corresponding to P_{max}. The yield displacement Δ_y for all specimens was determined by extrapolation from measured vertical displacement at $0{\cdot}75P_n$ in the 1% drift cycle (Hwang *et al.*, 2005; Lee and Ko, 2007). The strength parameters among different specimens are reported and compared in Table 1. The increase in displacement ductility from specimens J4–J7–J8 is not because of increase in ultimate displacement (Δ_{max}), but due to yield displacement (Δ_y). Higher stiffness of ascending hysteresis curves of respective specimens caused decrease in yield displacement (Δ_y). Specimen J9 exhibited large displacement ductility owing to proper anchorage and an effective joint shear-resisting mechanism.

6.5 Stiffness

Secant stiffness was used to provide a qualitative measure of the stiffness degradation in the specimens. In each cycle, secant stiffness was the slope of a line drawn between the maximum positive displacement point in the first half of the cycle to the maximum negative displacement point in the second half of the cycle. In Figure 8, the degradation of the secant stiffness is plotted against the corresponding cycle numbers for each specimen tested. A similar trend of stiffness degradation with increased displacement cycle is observed for all specimens. In specimen J9, many new cracks appeared, while earlier cracks propagated further in the fifth cycle, with rapid degradation of stiffness being observed in this cycle. The modes of failure for all specimens are reported in Table 2.

6.6 Effect on shear strength-

The maximum joint shear, $V_{jh,test}$, was obtained from the maximum applied load using

$$8. \quad V_{jh,test} = T_{max} - V_{col} = P_{max}\left[\frac{L_b}{jd} - \frac{(L_b + 0{\cdot}5h_c)}{L_c}\right]$$

where T_{max} is the maximum tensile force in the longitudinal reinforcement of the beam; V_{col} is the horizontal column shear in equilibrium with applied loading; and L_b is the length of the beam from the column face. Table 2 shows $V_{jh,test}$ values for all specimens.

In specimen J4, when joint shear capacity fell below the joint shear demand due to applied load at DR 4%, the joint failed in shear with the formation of a plastic hinge at the centre of the joint core. Detailing of the joint with joint hoops enhanced the shear capacity to greater than the demand and, hence, the strength of the specimen was defined by beam flexure capacity with formation of a plastic hinge at the beam interface.

The strength ratio of maximum joint shear to nominal shear strength ($V_{jh,test}/V_n^{ACI}$) for all specimens is compared in Table 2. ACI 318-08 (ACI, 2008) considers nominal shear strength as a function of concrete strength irrespective of the amount of shear reinforcement. The test results indicate that an increase in the amount of joint hoops increased the strength ratio ($V_{jh,test}/V_n^{ACI}$) from 0·78 to 0·89. Hence, it is necessary to define the contribution of transverse reinforcement while resisting horizontal shear force.

Specimen	$\frac{A_{sh,prod}}{A_{sh}^{318}}$	Ultimate load, P_{max}: kN		Maximum joint shear, $V_{jh,test}$: kN	$\frac{V_{jh,test}}{V_n^{318}}$	Mode of failure
		Upward direction	Downward direction			
J4	0	36·90	35·20	128·0	0·78	JF
J7	0·16	38·70	35·90	133·9	0·82	BJF
J8	0·5	40·20	38·40	139·4	0·85	BF
J9	1·0	41·80	39·20	145·0	0·89	BF

Table 2. Ultimate load, joint shear strength and mode of failure of specimens

Based on the capacity design concept, the estimated design shear force, $V_{jh,u}$ (Equation 7) is 141 kN for all the specimens. The maximum shear forces resisted by specimens J8 and J9 are almost equal to the estimated shear forces. Specimens J4 and J7 exhibited 9% and 5% less shear force in comparison with estimated shear force. All the parameters (crack pattern, hysteresis behaviour, modes of failure, energy dissipation, displacement ductility) studied indicate that the amount of joint hoops affects the global response of the beam–column joint, particularly at high inelastic cyclic load reversals when shear demand at a junction approaches the shear capacity of the joint. The amount of joint hoops provided in specimen J8 is sufficient to shift the location of the plastic hinge from the joint region to the beam interface. Park and Paulay (1974) suggested that, when the axial compression on the column is small (less than 12% of concrete capacity), the contribution of the concrete shear resistance should be ignored. In a reinforced concrete structure where concrete slabs are provided, the share of dead load is considerable in the column axial load. Hence, the role of the diagonal compression strut mechanism while resisting joint shear is significant.The headed bar had the advantage of transfer of more uniform distribution of compressive stress to the concrete at the headed end. This enables the development of a wider compressive strut in the joint, which enhances the joint shear strength. This finding suggests the possibility for a reduction of joint transverse reinforcement when using headed bars as longitudinal beam reinforcement.

Increased load reversals lead to distortion of the joint core, which develops tensile stress in the joint hoops. At this stage, joint hoops start contributing to resisting horizontal shear force. If the tensile stress in the joint hoops is restricted within elastic limits, effective crack control is possible. This will also retard the softening process of cracked concrete. Besides confining, the shear resisting mechanism at the joint core must be used while designing joint transverse reinforcement. Further investigations are required to establish the equation for defining the amount of joint transverse reinforcement when using headed bars by considering joint shear demand. It is also necessary to define the contribution of transverse reinforcement while resisting horizontal shear force.

7. Conclusion

This experimental study was conducted to investigate the role of joint hoops on the shear strength of exterior beam–column joints by using headed bars, and to assess the anchorage strength of headed bars with short development length. The tests were performed on four exterior beam–column joint specimens with varying amount of joint hoops. The test specimens were subjected to reverse cyclic loading. Based on the test results, the following conclusions are drawn.

- The provision of headed bars with head size $(A_{brg}/A_b) = 4$ and embedded length $(0 \cdot 12 f_y d_b / \sqrt{f'_c})$ was effective up to DR 3%, provided that the heads were placed within the diagonal compression strut of the joint. At higher DRs, the role of joint hoops is vital.
- The amount of joint hoops affects the global response of the beam–column joint, particularly at high inelastic cyclic load reversals when shear demand at the junction approaches the shear capacity of the joint.
- The headed bar had the advantage of transfer of more uniform distribution of compressive stress to the concrete at the headed end. This enables the development of a wider compressive strut in the joint, which enhances the joint shear strength. This finding suggests the possibility for a reduction of joint transverse reinforcement when using headed bars as longitudinal beam reinforcement.
- Further investigations are required to establish the equation for defining the amount of joint transverse reinforcement when using headed bars by considering joint shear demand. It is also necessary to define the contribution of transverse reinforcement while resisting horizontal shear force.

REFERENCES

ACI (American Concrete Institute) (2008) *Committee 318: Building Code Requirements for Structural Concrete and Commentary*. ACI, Farmington Hills, MI, USA, ACI 318-08.

ACI-ASCE (2002) *Committee 352: Recommendations for Design of Beam–Column Connections in Monolithic Reinforced Concrete Structures*. ACI, Farmington Hills, MI, USA, ACI 352R.

Bashandy TR (1996) *Application of Headed Bars in Concrete Members*. PhD thesis, University of Texas at Austin, Austin, TX, USA.

BIS (Bureau of Indian Standards) (1970) IS 383-1970 (reaffirmed 1997): Specification for coarse and fine aggregates from natural sources for concrete. Bureau of Indian Standards, New Delhi, India.

BIS (1991) IS 1489-1991: Portland pozzolana cement-specifications, Part 1 – Fly ash based. Bureau of Indian Standards, New Delhi, India.

Chun SC, Bohwan O and Naito CJ (2009) Anchorage strength and behaviour of headed bars in exterior beam–column joints. *ACI Structural Journal* **106(5)**: 579–590.

Chun SC, Lee SH, Kang THK, Oh B and Wallace JW (2007) Mechanical anchorage in exterior beam–column joints subjected to cyclic loading. *ACI Structural Journal* **104(1)**: 102–112.

Dhake PD, Patil HS and Patil YD (2015) Anchorage behaviour and development length of headed bars in exterior beam–column joints. *Magazine of Concrete Research* **67(2)**: 53–62.

Hwang SJ, Lee HJ, Liao TF, Wang KC and Tsai HH (2005) Role of hoops on shear strength of reinforced concrete beam–column joints. *ACI Structural Journal* **102(3)**: 445–453.

Kang THK, Ha SS and Choi DU (2010) Bar pullout tests and seismic tests of small-headed bars in beam-column joints. *ACI Structural Journal* **107(1)**: 32–42.

Kotsovou G and Mouzakis H (2011) Seismic behaviour of RC external joints. *Magazine of Concrete Research* **63(4)**: 247–264.

Lee HJ and Ko JW (2007) Eccentric reinforced concrete beam–column connections subjected to cyclic loading in principal directions. *ACI Structural Journal* **104(4)**: 459–467.

Park R and Paulay T (1974) The art of detailing. In *Reinforced Concrete Structures*. Wiley, New York, USA, pp. 716–759.

Scarpas A (1981) *The Inelastic Behaviour of Earthquake Resistant Reinforced Concrete Exterior Beam–Column Joints*. Department of Civil Engineering, University of Canterbury, Christchurch, New Zealand, research report.

Thompson MK, Ziehi MJ, Jirsa JO and Breen JE (2005) CCT nodes anchored by headed bars – Part I: Behaviour of nodes. *ACI Structural Journal* **102(6)**: 808–815.

Wallace JW, McConnell SW, Gupta P and Cote PA (1998) Use of headed reinforcement in beam–column joints subjected to earthquake loads. *ACI Structural Journal* **95(5)**: 590–606.

Wright JL and McCabe SL (1997) *The Development Length and Anchorage Behaviour of Headed Reinforcing Bars*. The University of Kansas, Center for Research, Lawrence, Kansas, SM report no. 44, Structural Engineering and Engineering Materials.